Statistical properties of actions of periodic orbits

Mitsusada M. Sano[a]

Department of Fundamental Sciences, Faculty of Integrated Human Studies, Kyoto University, Sakyo-ku, Kyoto, 606-8501, Japan

We investigate statistical properties of unstable periodic orbits, especially actions for two simple linear maps (p-adic Baker map and sawtooth map). The action of periodic orbits for both maps is written in terms of symbolic dynamics. As a result, the expression of action for both maps becomes a Hamiltonian of one-dimensional spin systems with the exponential-type pair interaction. Numerical work is done for enumerating periodic orbits. It is shown that after symmetry reduction, the dyadic Baker map is close to generic systems, and the p-adic Baker map and sawtooth map with noninteger K are also close to generic systems. For the dyadic Baker map, the trace of the quantum time-evolution operator is semiclassically evaluated by employing the method of Phys. Rev. E **49**, R963 (1994). Finally, using the result of this and with a mathematical tool, it is shown that, indeed, the actions of the periodic orbits for the dyadic Baker map with symmetry reduction obey the uniform distribution modulo 1 asymptotically as the period goes to infinity. © *2000 American Institute of Physics.* [S1054-1500(00)02101-7]

Recent development of semiclassical quantization of chaotic systems has given us many fruitful results and has been applied to mesoscopic systems, atom-molecular systems, nuclear systems, etc. One of the most important goals of theoretical research is to elucidate the relation between the prediction of random matrix theory and the statistical behavior of quantized chaotic systems. To develop semiclassical reasoning for this, it is quite important to know the statistical behavior of periodic orbits of the classical counter part. In this paper, we investigate the action of periodic orbits for simple two-dimensional maps (Baker map and sawtooth map) theoretically and numerically and report their statistical properties (e.g., Gaussian distribution and uniform distribution). In particular, as a main result, for dyadic Baker map with symmetry reduction, mathematical discussion supports the uniform distribution modulo 1 of actions of periodic orbits.

I. INTRODUCTION

Complex motion in chaotic dynamics is, in some sense, due to infinite number of variations of how a given system behaves. Infinite variations prevent us from forecasting the future of the system in detail. The set of unstable periodic orbits (UPOs), which is an countably infinite invariant set in chaotic dynamics, is regarded as a generator of an infinite number of variations. In fact, the dynamical property of the hyperbolic system is described by the dynamical zeta function (or the Fredholm determinant of the Perron–Frobenius operator), which is expressed in terms of information on UPOs.[1,2] The dynamical zeta function provides us with the dynamical characteristic quantities, such as decay rate, Lyapunov exponent, topological entropy, etc.[1]

The UPOs are also important objects for the purpose of quantizing chaotic systems. The eigen energies are formed as a result of complicated interference of waves along the UPOs, while for the regular system simple quantization condition, i.e., the Einstein–Brillouin–Keller quantization condition, is applied to the torus in classical dynamics. For quantized chaotic systems, this complicated feature of interference is encoded in the Gutzwiller trace formula or the associated Gutzwiller–Voros zeta function in a semiclassical way. The most striking property of a quantized chaotic system is good agreement with the prediction of the random matrix theory (RMT), which assumes an ensemble of Hamiltonian matrices according to the symmetry which a given system possesses. Even though the RMT gives us nice description for quantized chaotic systems, randomness deterministically generated in such systems is highly nontrivial. The link between classical chaos and the RMT should be clarified. A recent detailed investigation by semiclassical theory has shown that the statistical property of the UPOs determines the statistical property of the corresponding quantum system.

Here we briefly comment on known statistics of periodic orbits. The number of the periodic orbits exponentially proliferates with increasing their period,[3]

$$\#\{T_p \leqslant T\} \sim \frac{e^{hT}}{hT}, \tag{1}$$

where h is the topological entropy. For dispersing billiard systems, a numerical calculation shows that the length and stability factor for the set of periodic orbits with the same number of bounces obey the Gaussian distribution.[4] Moreover, the nearest neighbor spacing distribution for the length of periodic orbits approximately obeys the Poisson process.[4] In fact, this statistic explains linearity of the spectral form factor for a quantum dispersing billiard in a short time regime.[5]

For the correspondence between the behavior of a quantized chaotic system and the prediction of the RMT, the two-point level correlation function $R_2(s)$ is the most suitable characteristic function. For this quantity, MIT group,[6] and Bogomolny and Keating[7] (see Appendix A for a brief review) have obtained an apparently complete answer. However, their result has excellent agreement with the RMT prediction for the class of time-broken symmetry for both limit $s \to \infty$ and 0 (it seems to be a complete answer), but does not reproduce the RMT result in $s \to 0$ for the class of time-reversal symmetry. This failure is as follows: as $s \to 0$, the diagonal part $R_2^{(\text{diag})}(s)$ diverges. This divergence is due to the Hannay–Ozorio de Almeida (H–OdA) sum rule,[8,9] which represents a tendency toward a unique equilibrium state in the corresponding classical dynamics. For time-broken symmetry, the off-diagonal part $R_2^{(\text{off})}(s)$ also diverges and cancels the divergence in $R_2^{(\text{diag})}(s)$. For time-reversal symmetry, this cancellation does not occur for their result, because the order of divergence in $R_2^{(\text{diag})}(s)$ mismatches that in $R_2^{(\text{off})}(s)$ (see Appendix A). $R_2^{(\text{off})}(s)$ contains the information on the pair correlation of UPOs.[10] This correlation is highly nontrivial and shows the deviation from pure randomness. As shown for the Riemann zeta function which is a mathematical test model of a quantized chaotic system by Keating,[11,12] the cancellation between the divergence in $R_2^{(\text{diag})}(s)$ and that in $R_2^{(\text{off})}(s)$ is essential to its deviation. In order to improve their result, time-reversal symmetry breaking of $R_2(s)$ has been considered in Ref. 13 by careful treatment of multiplicity of UPOs. The result of Ref. 7 has been partially improved but this problem still remains.

In the analysis of Ref. 7, the crucial statistical assumption has been made: the distribution of actions obeys Gaussian distribution and the distribution of actions modulo 1 (in the scale unit of $\hbar$) obeys uniform distribution. In the present paper, we will investigate the statistical property of actions of the UPOs for two simple examples of hyperbolic dynamical systems, a Baker map, and a sawtooth map. Our aim here is to check whether actions for both maps obey the assumptions, which has been used in Ref. 7, or not. We use the recent numerical result by Tanner[14] in which he applied the result of Ref. 15 to the action correlation, and an extension of Weyl's uniform distribution theorem. As a result, it will be shown that a dyadic Baker map with a symmetry reduction obeys the uniform distribution of actions modulo 1. A p-adic Baker map and a sawtooth map are also investigated numerically. From the numerical result for these cases, it seems that for the p-adic Baker map and special cases of the sawtooth map, actions of UPOs obey the uniform distribution modulo 1.

The organization of this paper is as follows: In Sec. II, we introduce dyadic Baker map and write the expression of action for UPOs into the form of a Hamiltonian of one-dimensional lattice gas system by using the binary symbolic dynamics. In Sec. III, the quantized dyadic Baker map is introduced. We carry out the semiclassical theory to the trace of its Floquet operator. The evaluation of the semiclassical trace is reduced to the evaluation of eigenvalues of some operator. The behavior of this eigenvalues determines the

statistical property of actions. The numerical results of action distribution are displayed. It will be shown that the dyadic Baker map with a symmetry reduction seems to satisfy the assumption in Ref. 7. In Sec. IV, we consider the action distribution of a dyadic Baker map rather mathematically, but not strictly rigorously. Using the similarity between the semiclassical trace (the sum over periodic orbits) and the sum which appears in Weyl's uniform distribution theorem, we will confirm that the actions of UPOs of a dyadic Baker map with symmetry reduction obey the uniform distribution modulo 1. In Sec. V, we will consider the case of the sawtooth map. It is shown that the expression of actions for UPOs becomes the Hamiltonian of a one-dimensional Potts model. In Sec. VI, we summarize the conclusions. In Appendix A, the result on the semiclassical expression of $R_2(s)$ is given. The validity of the semiclassical sum rule is checked for both time-reversal and time-broken cases. In Appendix B, we represent the resummation method to the dyadic Baker map which is originally employed by Gutzwiller to the anisotropic Kepler problem. In Appendix C, the extension to the p-adic Baker map is done.

II. DYADIC BAKER MAP

The dyadic Baker map is the area-preserving map on a unit square,

$$x' = 2x - [2x],$$
$$y' = \frac{y + [2x]}{2}. \tag{2}$$

The orbit can be expressed in terms of the binary series,

$$x = \sum_{i=0}^{\infty} a_i \left(\frac{1}{2}\right)^{i+1}, \quad y = \sum_{i=0}^{\infty} b_i \left(\frac{1}{2}\right)^{i+1}, \tag{3}$$

where $a_i, b_i \in \{0,1\}$. The bi-infinite symbolic sequence,

$$(\cdots b_n b_{n-1} \cdots b_2 b_1 \bullet a_0 a_1 a_2 \cdots a_n \cdots), \tag{4}$$

specifies an actual orbit. This correspondence is one-to-one.

The generating function of the Baker map can be constructed by the following way through the mixed representation.[16] Let us consider the generating function for the T-step mapping. The T-step mapping is given as

$$x' = 2^T x - \nu,$$
$$y' = 2^{-T}(y + \bar{\nu}). \tag{5}$$

Therefore, the associated generating function is now

$$F_\nu(x, y') = 2^T y' x - \nu y' - \bar{\nu} x, \tag{6}$$

where

$$\nu = \sum_{i=0}^{T-1} a_i 2^{T-i-1}, \quad \bar{\nu} = \sum_{i=0}^{T-1} a_i 2^i. \tag{7}$$

The mapping is expressed in terms of this generating function,

$$x' = \frac{\partial F_\nu}{\partial y'} = 2^T x - \nu, \quad y = \frac{\partial F_\nu}{\partial x} = 2^T y' - \bar{\nu}. \tag{8}$$

For periodic orbits, we identify the initial point and final point, namely $x = x'$, $y = y'$. Then, we get the position of the periodic point,

$$x^* = \frac{\nu}{2^T - 1},$$

$$y^* = \frac{\bar{\nu}}{2^T - 1}.$$

(9)

We also denote the one-step shift by σ and define here the shifted periodic sequence $\sigma^n \nu$,

$$\sigma^n \nu = \sum_{i=0}^{T-1} a_{(i+n) \bmod T} 2^{T-i-1}.$$

(10)

There is an interesting property of periodic points: The sums of x_n and y_n are the sum of the symbols a_n's,

$$\sum_{n=0}^{T-1} x_n = \sum_{n=0}^{T-1} y_n = \sum_{n=0}^{T-1} a_n.$$

(11)

A similar relation will appear for the sawtooth map later. The action of the periodic orbit is obtained by the Legendre transformation of the generating function F_ν,

$$S_\nu = y'x' - F_\nu(x, y')|_{x^*, y^*} = \frac{\nu \bar{\nu}}{2^T - 1}.$$

(12)

We denote the set of the actions of the periodic orbits with period T by $\mathcal{PO}_T$ which includes all repetitions, namely $T = rT_p$, where r is the repetition and T_p is the period of the prime periodic orbits labeled by p. We also denote the set of the actions S_ν for the prime periodic orbits with period T by $\mathcal{P}_T$.

Subtracting some integer from S_ν, the expression of S_ν is much more simplified. We define $\overline{S_\nu} \equiv S_\nu - \mathcal{I}_\nu$, where $\mathcal{I}_\nu = \Sigma_{j=0}^{T-1} a_j 2^{T-1-j}$,

$$\overline{S_\nu} \equiv \sum_{i=0}^{T-1} x_i a_i = \sum_{i=0}^{T-1} x_i [2x_i],$$

(13)

where

$$x_n = \frac{\sigma^n \nu}{2^T - 1},$$

(14)

and

$$M_\nu = \sum_{i=0}^{T-1} a_i, \quad \frac{M_\nu}{2} \leq \overline{S_\nu} < M_\nu.$$

(15)

Obviously, $S_\nu \bmod 1 = \overline{S_\nu} \bmod 1$. We use this expression $\overline{S_\nu}$ rather than the original S_ν, since in semiclassical analysis we only need the fractional part of S_ν, as we will see later. Here we denote the set of the actions $\overline{S_\nu}$ with period T by $\overline{\mathcal{PO}_T}$ (for the prime periodic orbits, $\overline{\mathcal{P}_T}$.). $\overline{S_\nu}$ can be written as

TABLE I. Symmetry operations and minimum degeneracy.

σ_T	σ_R	g
×	×	1
×	○	2
○	×	2
○	○	4

$$\overline{S_\nu} = \sum_{i=0}^{T-1} x_i a_i$$

$$= \frac{2^{T-1}}{2^T - 1} \sum_{i=0}^{T-1} \sum_{j=0}^{T-1} 2^{-j} a_i a_{(i+j) \bmod T}$$

$$= \frac{e^{\lambda T/2}}{4 \sinh(\lambda T/2)} \left\{ \sum_{i=0}^{T-1} a_i^2 + 2 e^{-\lambda T/2} \sum_{i<j} a_i a_j \right.$$

$$\left. \times \cosh\left[\lambda \left(\frac{T}{2} - |i-j| \right) \right] \right\},$$

(16)

where $\lambda = \ln 2$. Finally the action $\overline{S_\nu}$ can be rewritten into the one-dimensional lattice gas Hamiltonian with system size T,

$$\overline{S_\nu} = \frac{e^{\lambda T/2}}{4 \sinh(\lambda T/2)} \left\{ M_\nu + e^{-\lambda T/2} \sum_{i \neq j} a_i a_j \right.$$

$$\left. \times \cosh\left[\lambda \left(\frac{T}{2} - |i-j| \right) \right] \right\},$$

(17)

where M_ν denotes the number of particles (i.e., the number of "1"). This is very similar to the approximate action of periodic orbits for the anisotropic Kepler problem which is an Ising spin system with exponentially decreasing pair interaction.[17]

Symmetry: The Baker map has the following two types of symmetry. Under the following symmetry operation, the action $\overline{S_\nu}$ is invariant. (1) **Time-reversal operation:** This symmetry operation is the exchange of the coordinates x and y, namely $x \leftrightarrow y$. Let us represent this operation by σ_T. In the symbolic representation, it is given as $\overline{a_0 a_1 \cdots a_{T-1}} \leftrightarrow \overline{a_{T-1} a_{T-2} \cdots a_0}$. (2) **Geometrical symmetry (the reflection wrt the diagonal):** In the coordinate representation (x, y), this operation is given as $x \rightarrow 1-x$, $y \rightarrow 1-y$. Let us denote this operation by σ_R. In the symbolic representation, this operation is the posi-nega transformation. $\overline{a_0 a_1 \cdots a_{T-1}} \rightarrow \overline{(1-a_0)(1-a_1) \cdots (1-a_{T-1})}$. By these two symmetries, the multiplicity g of a given periodic orbit can be, at most, $g = 4$, except accidental degeneracy (we will observe accidental degeneracy in Fig. 5 and Fig. 6). The correspondence between the multiplicity and the symmetry operation is depicted in Table I.

An example of $g = 4$ for period 7. Here we show an example of degeneracy of prime periodic orbits with $g = 4$ (period 7). We list the symbols for an example case. (a) 0001011, (b) 0001101, (c) 0010111, (d) 0011101. (a) and (b) [or (c) and (d)] are mutually transformed by σ_T. At the same time, (a) and (d) [or (b) and (c)] are mutually transformed by σ_R.

III. QUANTIZED BAKER MAP

The quantized version of the Baker map is constructed in the following way.[18,19] Let us denote $\psi = (\psi_0, \psi_1, \ldots, \psi_{N-1})^T$ the wave function in the position representation. The time-evolution of the wave function is described by the following $N \times N$-matrix B_N (N: positive even integer),

$$B_N = G_N^{-1} \begin{pmatrix} G_{N/2} & \mathbf{0} \\ \mathbf{0} & G_{N/2} \end{pmatrix}, \tag{18}$$

where

$$(G_N)_{kn} = \langle k | n \rangle = \frac{1}{\sqrt{N}} \exp\left[-\frac{2\pi i}{N}\left(k + \frac{1}{2}\right)\left(n + \frac{1}{2}\right)\right],$$

$$k, n = 0, 1, \ldots, N-1. \tag{19}$$

The phase space is now compact. This makes the Planck constant be quantized to give $\hbar = 1/2\pi N$, where N is the integer which corresponds to the size of matrix B_N. The eigenvalue problem is now

$$B_N \psi = e^{i\omega} \psi. \tag{20}$$

The quantized Baker map shows the level repulsion. The nearest-neighbor level spacing distribution well agrees with the Wigner distribution for $N \neq 2^L$.[18] For the case of $N = 2^L$, the accidental degeneracy of quasi-energies is observed. This curious property is not yet well understood. We will see later for the numerical result of a spectral form factor. Since the eigenvalue is periodic with period 2π, then the density of states is represented in terms of the sum of infinite number of delta functions,

$$d(\omega) = \sum_{n=1}^{N} \sum_{l=-\infty}^{+\infty} \delta(\omega - \omega_n - 2\pi l)$$

$$= \frac{N}{2\pi} + \frac{1}{\pi} \Re \sum_{n=1}^{\infty} \mathrm{Tr}(B_N^n) e^{-in\omega}. \tag{21}$$

The first term in the second line corresponds the mean density of states $\bar{d} = N/2\pi$. To characterize the statistical property of spectrum, we define the two-point correlation function $R_2(s)$,

$$R_2(s) \equiv \frac{1}{\bar{d}^2} \left\langle \tilde{d}\left(\omega + \frac{s}{2\bar{d}}\right) \tilde{d}\left(\omega - \frac{s}{2\bar{d}}\right)\right\rangle_\omega$$

$$= \frac{1}{2\pi \bar{d}^2} \int_0^{2\pi} d\omega \, \tilde{d}\left(\omega + \frac{s}{2\bar{d}}\right) \tilde{d}\left(\omega - \frac{s}{2\bar{d}}\right), \tag{22}$$

where $\tilde{d}(\omega) = d(\omega) - \bar{d}$ and $\langle \cdots \rangle$ denotes the energy average. The spectral form factor $K(T;N)$ is defined as the Fourier transform of the two-point level correlation function,
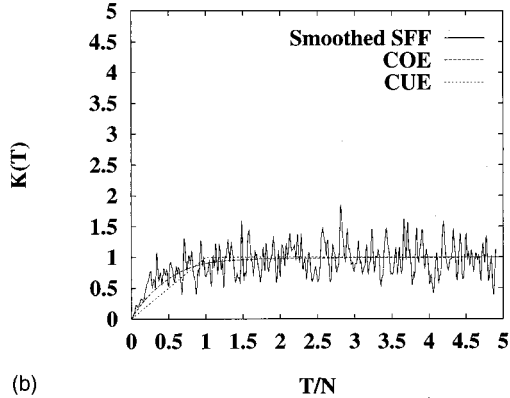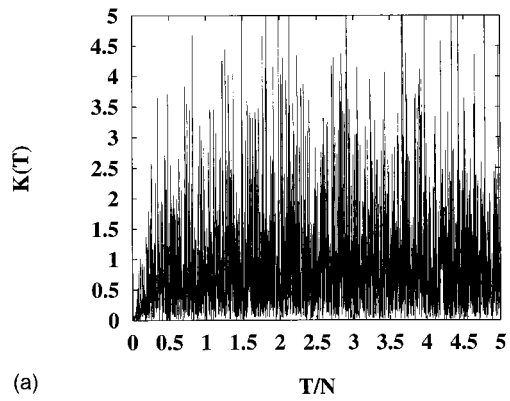

FIG. 1. Spectral form factor of a quantized dyadic Baker map: $N = 1/2\pi\hbar = 1000$. We used half of the whole eigenvalues, which corresponds to the even parity. The horizontal axis is in scale T/N. $t_H = T/N = 1$ is the Heisenberg time. (a) The spectral form factor. (b) The smoothed spectral form factor which is obtained by smoothing (a) in a certain small interval. The solid line is the quantized dyadic Baker map. The dashed and dotted lines are the COE and CUE statistics, respectively.

$$K(T;N) = \int_0^{2\pi \bar{d}} ds \, e^{iTs/\bar{d}} R_2(s)$$

$$= \frac{1}{2\pi \bar{d}^2} \int_0^{2\pi \bar{d}} ds \, e^{iTs/\bar{d}} \int_0^{2\pi} \tilde{d}\left(\omega + \frac{s}{2\bar{d}}\right) \tilde{d}\left(\omega - \frac{s}{2\bar{d}}\right)$$

$$= \frac{1}{N} |\mathrm{Tr}(B_N^T)|^2 - N\delta_{T0}. \tag{23}$$

The random matrix theory predicts the form of $K(T;N)$ for time-reversal ($g = 2$) and for time-broken systems ($g = 1$), respectively,

$$K_{g=2}(T;N) = \begin{cases} 2t - t\ln(1+2t), & 0 < t \leq 1, \\ 1 - t\ln\left(\dfrac{2t+1}{2t-1}\right), & 1 < t, \end{cases} \tag{24}$$

and

$$K_{g=1}(T;N) = \begin{cases} t, & 0 < t \leq 1, \\ 1, & 1 < t, \end{cases} \tag{25}$$

where we take the scale $t = T/N$. In Fig. 1 and Fig. 2, the numerical results of the spectral form factor for even parity are depicted for $N = 1000$ and $N = 1024 = 2^{10}$, respectively. Figure 1 shows good agreement with the COE prediction, while Fig. 2 seems to be rather Poisson, i.e., arithmetical
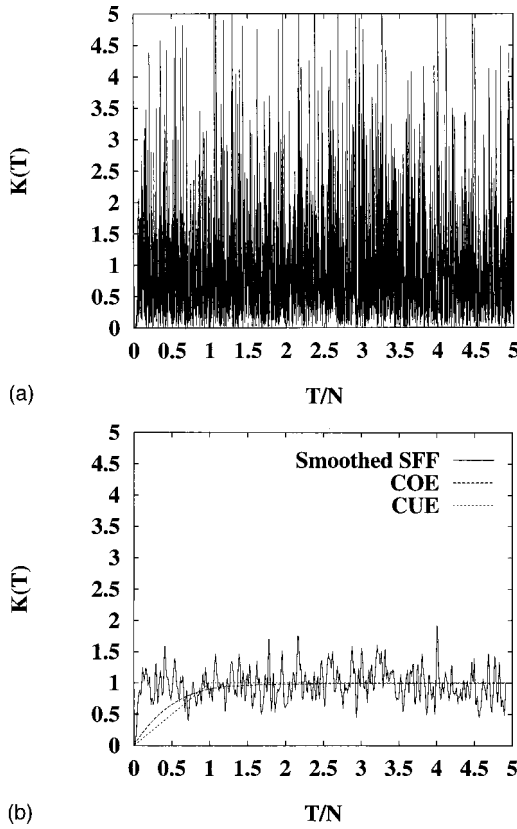
FIG. 2. Spectral form factor of a quantized Baker map (arithmetical case): $N = 1/2\pi\hbar = 2^{10} = 1024$. We used half of the whole eigenvalues, which corresponds to the even parity. The horizontal axis is in scale T/N. $t_H = T/N = 1$ is the Heisenberg time. (a) The spectral form factor for $N = 1024$. (b) The smoothed spectral form factor which is obtained by smoothing (a) in a certain small interval. The solid line is the Baker map. The dashed and dotted lines are the COE and CUE statistics, respectively.

chaos.[20] This observation is consistent with the numerical result of the level spacing distribution in Ref. 14. Thus we must carefully treat the $\hbar$-(or N-)dependence. If there is no systematic degeneracy in eigenenergies, the following semiclassical sum rule, Eq. (27), should be satisfied which is a simple application of identity on the smoothed delta functions:[8]

$$\lim_{\epsilon \to 0} 2\pi\epsilon \left(-\frac{1}{\pi}\Im\frac{1}{x+i\epsilon} \right)^2 = \delta(x). \tag{26}$$

The semiclassical sum rule is

$$\lim_{\epsilon \to 0} 2\pi\epsilon R_2^{(\epsilon)}(s=0) = \bar{d}, \tag{27}$$

where

$$R_2^{(\epsilon)}(s) = \frac{1}{2\pi\bar{d}^2}\int_0^{2\pi} d\omega \tilde{d}^{(\epsilon)}\left(\omega + \frac{s}{2\bar{d}}\right)\tilde{d}^{(\epsilon)}\left(\omega - \frac{s}{2\bar{d}}\right) \tag{28}$$

and $\tilde{d}^{(\epsilon)}(\omega)$ is the oscillatory part of an ϵ-Lorentzian smoothed density of states. The relation, Eq. (27), implies the discreteness of eigenenergies. Inserting Eq. (21) into Eq. (27), we have

$$\lim_{\epsilon \to 0} 2\epsilon \sum_{T=1}^{\infty} K(T;N) e^{-2\epsilon T} = 1. \tag{29}$$

This implies that the spectral form factor $K(T;N)$ saturates to 1 as $T \to \infty$.

The semiclassical trace can be evaluated as[16,21]

$$\text{Tr}^{(\text{sc})}(B_N^T) = \sum_{S_\nu \in \text{Fix}(T)}' \frac{e^{2\pi i N S_\nu}}{2\sinh(\lambda T/2)}, \tag{30}$$

where the sum is taken over the fixed points of the T-times map except $\overline{0}^T$ and $\overline{1}^T$ which lay on the discontinuous boundary. Fix(T) is the set of the actions of the fixed points with period T. We note that the Maslov index is absent for a quantized Baker map. The contribution from the periodic orbits $\overline{0}^T$ and $\overline{1}^T$ is of the order of $\log(\hbar)$.[21] In the semiclassical limit $\hbar \to 0$, this anomaly has a problem. One can avoid this problem by using the different Baker map.[22] For the Baker map of Ref. 22, the action is just $\frac{1}{4}$ of S_ν and we can enumerate all periodic orbits by the same binary symbolic dynamics. But in this paper, since we are interested in the statistics of the actions, we sum up all contributions from the symbols $\overline{0}$ and $\overline{1}$. For the usual Baker map, we sum up all contribution apart from the symbols. Semiclassically the spectral form factor can be written as

$$K^{(\text{sc})}(T;N) \equiv \frac{1}{N}|\text{Tr}^{(\text{sc})}(B_N^T)|^2$$

$$= \frac{1}{N\{2\sinh(\lambda T/2)\}^2}$$

$$\times [gT2^T + (\text{other contribution})], \tag{31}$$

where the first term 2^T in the bracket is the number of periodic orbits with period T and g is the degeneracy of the periodic orbits. ($g = 2$ for a symmetry reduced Baker map, $g = 4$ for the not symmetry reduced one). The H–OdA sum rule is satisfied.[9] Considering the multiplicity of periodic orbits due to the time-reversal symmetry, the diagonal part explains the slope of $K(T;N)$ in a short time limit, namely the linearity in T.[8] On the other hand, in the long time limit, however, the saturation of $K(T;N)$ needs the off-diagonal part which expresses the correlation of actions. Unfortunately, the semiclassical spectral form factor exponentially diverges.[23,14] So the semiclassical sum rule also breaks down for the semiclassical two-point level correlation function $R_2(s)$. Although the semiclassical spectral form factor diverges, it is worthwhile examining the explicit enumeration of the off-diagonal part. In addition, as pointed out in Ref. 23, the divergence of the semiclassical spectral form factor is controlled by the imaginary part of the semiclassical eigenenergies. The semiclassical trace $\text{Tr}^{(\text{sc})}(B_N^T)$ diverges as $\sim e^{\lambda T/2}$, where $h_{\text{top}} - \lambda/2 (=\lambda/2$ in the present case) is the topological barrier and λ is the maximum Lyapunov exponent ($= \ln 2$ for the dyadic Baker map). Conversely, in order to obtain the semiclassical sum rule for the semiclassical two-point correlation or the saturation of the semiclassical form factor in $T \to \infty$, we need the energy smoothing with the size of $\lambda/2$ at least. So if we have an explicit expression of

$K^{(\mathrm{sc})}(T;N)$, equivalently the trace $\mathrm{Tr}^{(\mathrm{sc})}(B_N^T)$, there is a possibility to control the imaginary part of eigenenergies, i.e., exponential rate of divergence, by hand. The action correlation can be expressed by the following quantity $P(y;n)$,[10,14]

$$P(y;T) = \sum_{N=-\infty}^{\infty} |\mathrm{Tr}^{(\mathrm{sc})}(B_N^T)|^2 e^{2\pi i y N}, \tag{32}$$

where $N = 1/2\pi\hbar$. From this expression, it is clear that the $\hbar$-(or N-)dependence of $K^{(\mathrm{sc})}(T;N)$ is important. The RMT prediction for the action correlation[10,14] is as follows: for the GUE,

$$P_{\mathrm{GUE}}(\sigma) = \frac{1}{T^2} P\left(\frac{\sigma}{T}\right) = \frac{\bar{P}(T)}{T^2} - \left(\frac{\sin(\pi\sigma)}{\pi\sigma}\right)^2 + T\delta(\sigma), \tag{33}$$

and for the GOE,

$$\begin{aligned} P_{\mathrm{GOE}}(\sigma) &= \frac{1}{T^2} P\left(\frac{\sigma}{T}\right) \\ &= \frac{\bar{P}(T)}{T^2} - 2\left(\frac{\sin(\pi\sigma)}{\pi\sigma}\right)^2 \\ &\quad + \frac{2}{\pi\sigma}\{\cos(2\pi\sigma)(\mathrm{si}(2\pi\sigma)\cos(2\pi\sigma) \\ &\quad - \mathrm{Ci}(2\pi\sigma)\sin(2\pi\sigma)) + \mathrm{Ci}(4\pi\sigma)\sin(4\pi\sigma) \\ &\quad - \mathrm{si}(4\pi\sigma)s(4\pi\sigma)\} + 2\delta(\sigma), \end{aligned} \tag{34}$$

where we used the scaling $y = \sigma/T$ and $\bar{P}(y)$ corresponds the mean part of the weighted periodic orbit action pair density.[14]

Recently in Ref. 14, using the weighted Perron–Frobenius operator (WPF operator) $\mathbf{U}_N$ for the Baker map introduced in Ref. 15, the action correlation has been investigated. The definition of $\mathbf{U}_N$ is

$$\mathbf{U}_N(q,q';N) = \sqrt{2}\,\delta(q - (2q' - [2q']))e^{2\pi i N S(q')}, \tag{35}$$

where

$$S(q') = q'[2q'] - \tfrac{1}{2}([2q'] + q'). \tag{36}$$

The most striking thing is that the semiclassical trace of the Baker map can be replaced by the trace of the WPF operator $\mathbf{U}_N$ and the evaluation of the semiclassical trace is now the evaluation of eigenvalues of $\mathbf{U}_N$.[24] Thanks to this nice property, he could enumerate the semiclassical trace up to period 500. The semiclassical trace is given by

$$\mathrm{Tr}^{(\mathrm{sc})}(B^T) = \sum_{S_\nu \in \mathrm{Fix}(T)} \frac{e^{2\pi N S_\nu i}}{2\sinh(\lambda T/2)} = \mathrm{Tr}(\mathbf{U}_N^T) = \sum_{i=0}^{\infty} \Lambda_i^T(N), \tag{37}$$

where $\{\Lambda_i(N)\}_{i=0}^{+\infty}$ is the set of eigenvalues of $\mathbf{U}_N$. He has also shown that (1) the symmetry reduction (i.e., geometrical symmetry) is important; (2) to see the action correlation, the sum should be truncated; and (3) the unitarity enforced by using the bootstrap method[7] is important for the action correlation. The symmetry reduced semiclassical trace is given as
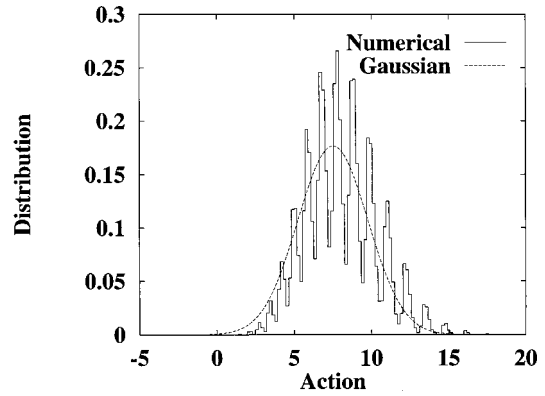

FIG. 3. Action distribution ($\bar{S}_\nu = \Sigma x_i[2x_i]$) for the prime periodic orbits with period 20 without symmetry reduction: The distribution is approximately Gaussian. The distribution has a periodic oscillation. Each peak is assigned by the number M_ν.

$$\begin{aligned} \mathrm{Tr}(B_{\pm,N}^T) = \frac{1}{2}\Bigg[&\frac{1}{2\sinh(\lambda T/2)} \sum_{S_\nu \in \mathrm{Fix}(T)} e^{2\pi i N S_\nu} \\ &\mp \frac{1}{2\cosh(\lambda T/2)} \sum_{S_\nu \in \mathrm{Fix}'(T)} e^{2\pi i N S_\nu'}\Bigg], \end{aligned} \tag{38}$$

where S_ν' corresponds to half action of an orbit with length $2T$ whose symbol sequence is given as $(a_0,\cdots,a_{T-1},1 - a_0,\cdots,1-a_{T-1})$ and $\mathrm{Fix}'(T)$ is the set of the actions S_ν' of the fixed points with period $2T$. $+$ (and $-$) corresponds to even (and odd) parity, respectively. In the next subsection, we will show the action distribution before symmetry reduction and after symmetry reduction.

What is the most important for us is that the numerical observation of the leading eigenvalue (i.e., maximum modulus) of $\mathbf{U}_N$ for each irreducible symmetry.[14] Assigning two irreducible representations by $+$ and $-$, the leading eigenvalues of $\mathbf{U}_N$ (i.e., the eigenvalue with the maximum absolute value) is greater than 1 and behave like

$$\log|\Lambda_0^{(\pm)}(N)| \simeq \frac{C}{\sqrt{N}}, \tag{39}$$

where $C \approx 0.29$.[15] The asymptotic behavior of the semiclassical trace and the spectral form factor. This fact will be used for a mathematical discussion in the next section.

We can also consider another quasiclassical operator like $\mathbf{U}_N$, i.e., the Gutzwiller's operator[17] in Appendix B. However, this method fails in the semiclassical limit. See Appendix B in details.

A. Numerical observation of action distribution

In this subsection, we show the numerical results for the action distribution of the periodic orbits for Baker maps. First, we depict the actual action distribution for the expression $\bar{S}_\nu$ without symmetry reduction in Fig. 3 [bare distribution ($\bar{S}_\nu$)] and Fig. 4 ($\bar{S}_\nu$ mod 1) for the prime periodic orbits. At first sight, the distribution has an oscillation of period ~ 1. It looks like the binomial distribution. Remember the assumption on the action distribution of the periodic orbits for their semiclassical analysis in Ref. 7. They assumed
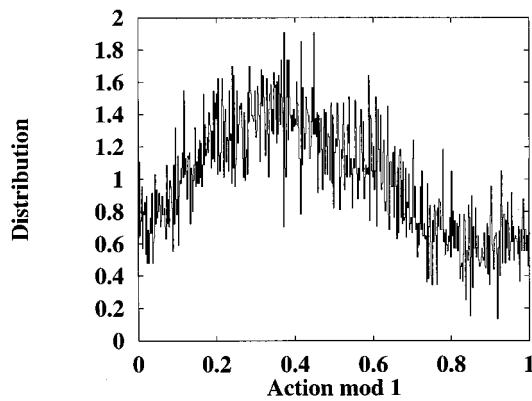
FIG. 4. Action distribution ($\bar{S}_\nu$ modulo 1) without symmetry reduction: for the prime periodic orbits with period 20. A remarkable feature is that the distribution has an oscillation in the unit interval.

FIG. 6. Multiplicity distribution of actions modulo 1 for the prime periodic orbits with period 20 without symmetry reduction: The vertical axis represents the multiplicity of actions. For a higher period, we observe high multiplicity.

that (1) the bare action of periodic orbits obeys Gaussian and (2) the actions modulo $\hbar$ of periodic orbits are uniformly distributed. From Figs. 3 and 4, the assumption seems to be invalid for Baker maps without symmetry reduction. In addition, at present, we do not know whether these peaks have the remarkable hierarchical structure as the case of the time-domain approach in Ref. 25.

Next we examine the degeneracy of the action of periodic orbits without symmetry reduction, which is extremely important for the behavior of the spectrum of the corresponding quantum system. We remember the symmetry relation of the action $\bar{S}_\nu$. (a) Time reversal operation: $\bar{S}_{\sigma_T \nu} = \bar{S}_\nu$; (b) posi-nega reverse operation: $\bar{S}_{\sigma_R \nu} = \bar{S}_\nu + T - 2M$; (c) shift by one-step: $\bar{S}_{\sigma \nu} = \bar{S}_\nu$, In Figs. 5 and 6, we represent the distribution of the multiplicity of actions. Each spike corresponds to the value of actions. Its height represents the multiplicity. Figure 5 is bare distribution for period 20. Higher degeneracies than $g = 4$ are observed. In Fig. 6, we depict the distribution of the multiplicity of actions modulo 1. After the modulo operation, multiplicity becomes much higher. It is numerically confirmed that the higher period has higher degeneracy. We summarize that the Baker map without symmetry reduction has the tendency of high degeneracy of actions.

The distribution of the pair-difference of the actions $[\bar{S}_\nu - \bar{S}_{\nu'}(\nu \neq \nu')]$ is depicted in Fig. 7(a) (bare distribution) and Fig. 7(b) (in modulo 1). For generic systems, the distribution of the pair-difference of the actions can be expected to be approximately Gaussian, since the action distribution is approximately Gaussian as assumed in Ref. 7. In Fig. 7(a), we depict the bare distribution of the pair-difference of the actions for period 17. Only the positive axis is shown. There exist some peaks in the distribution. The envelope function of the distribution seems to be Gaussian. Figure 7(b) shows

(a)

(b)

FIG. 7. Distribution of $S_\nu - S_{\nu'}(\nu \neq \nu')$ for prime periodic orbits (period 17) without symmetry reduction: (a) Bare distribution. We only show $S_\nu - S_{\nu'} > 0$. The distribution has the periodic peaks as well as in the action distribution. (b) Distribution modulo 1. The distribution has the periodic oscillation as well as in the action distribution with modulo operation.
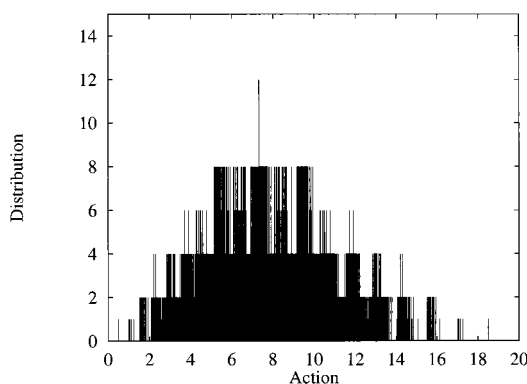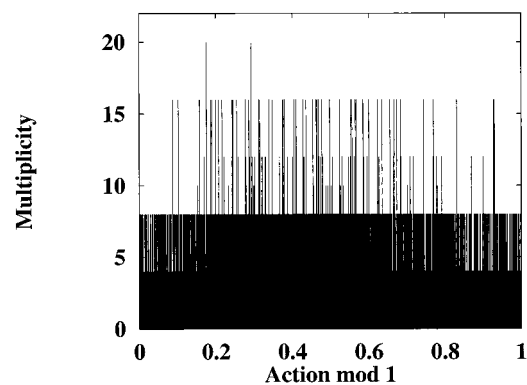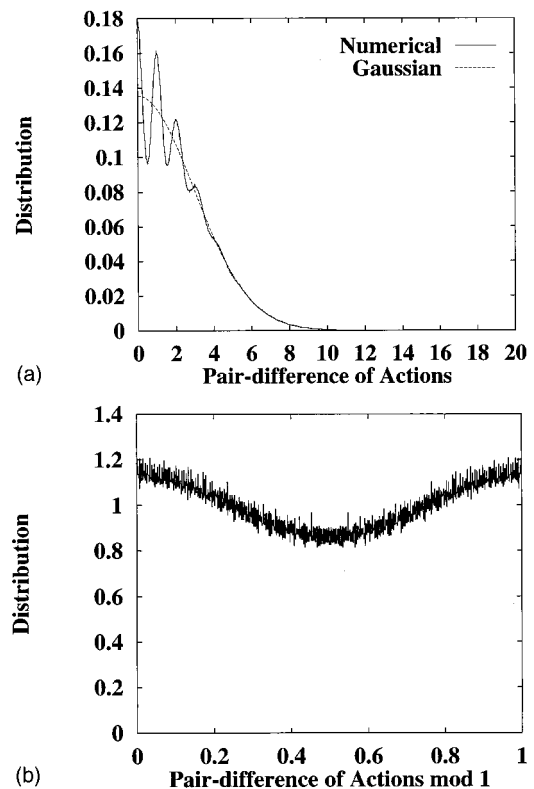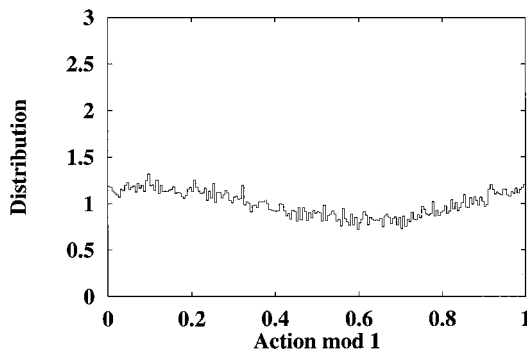

FIG. 5. Multiplicity distribution of the actions for prime periodic orbits with period 20 without symmetry reduction: The vertical axis represents the multiplicity. Higher degeneracies than $g = 4$ are observed.

FIG. 8. Action distribution (S_ν modulo 1) for the Baker map with symmetry reduction (odd parity) with period 22: The distribution is close to uniform distribution.

the distribution after the modulo 1 operation is depicted. Reflecting the tendency of the degeneracy of actions, the distribution is not uniform distribution. In summary, the dyadic Baker map has the tendency of high degeneracy of actions without symmetry reduction.

Finally, we depict the action distribution modulo 1 after symmetry reduction (odd parity) in Fig. 8 (period 22). Compared with Fig. 4, it seems that the distribution tends to the uniform distribution as increasing period T, although it still has modulation. In the next section, this point will be mathematically confirmed.

IV. DISTRIBUTION OF ACTIONS: MATHEMATICAL DISCUSSION

The expression of semiclassical trace for the dyadic Baker map is very similar to the sum which appears in Weyl's uniform distribution theorem. This manifests that for a dyadic Baker map, whether the distribution of actions is uniform or not is closely related to the value of its semiclassical trace. First, we introduce the definition of uniform distribution.

Definition: If the following condition is satisfied for a given infinite sequence of real number $\{a_n\}$, we say that it has uniform distribution modulo 1: for a given interval $E = [a,b] \subset I = [0,1]$,

$$\lim_{M \to \infty} \frac{A(E,M)}{M} = b - a, \tag{40}$$

where

$$A(E,M) = \#\{a_n : \{a_n\} \in E \quad for \quad n = 1,2,\dots,M\}, \tag{41}$$

and $\{a_n\}$ is the fractional part of a_n.

The uniform distribution is characterized by the following theorem.

Theorem: *The necessary and sufficient condition for the uniform distribution modulo 1 is the following: for an arbitrary Riemann integrable real function $f(x)$,*

$$\lim_{M \to \infty} \frac{1}{M} \sum_{n=1}^{M} f(\{a_n\}) = \int_0^1 f(x)dx. \tag{42}$$

Fortunately, one can set the function $f(x)$ to $\exp(2\pi i m x)$ (m: integer).

Weyl's uniform distribution theorem:[26] Consider a sequence of real number $\{a_n\}_{n=1}^{\infty}$. The necessary and sufficient condition that the fractional part $\{a_n\}$ of a_n is distributed uniformly in the interval $[0,1]$ is

$$\lim_{M \to \infty} \frac{1}{M} \sum_{n=1}^{M} \exp[2\pi i m a_n] = 0, \tag{43}$$

for an arbitrary natural number m.

The sum in Eq. (43) is very similar to the semiclassical expression of the trace for quantized chaotic linear maps. We have to extend the above Weyl's uniform distribution theorem to an appropriate form, i.e., the case of a sequence of sets of real numbers. We define the uniform distribution modulo 1 for this case.

Definition: For a given sequence of sets of real numbers, say, $\{\mathcal{S}\}_{n=1}^{\infty}$ such that $|\mathcal{S}_n| < |\mathcal{S}_{n+1}|$ and $|\mathcal{S}_n| \to \infty$, if the following condition is satisfied, we say that the elements of the set $\mathcal{S}_n$ has uniform distribution modulo 1 asymptotically: for an arbitrary interval $E = [a,b] \subset I = [0,1]$,

$$\lim_{n \to \infty} \frac{A(E,|\mathcal{S}_n|,\mathcal{S}_n)}{|\mathcal{S}_n|} = b - a, \tag{44}$$

and

$$A(E,|\mathcal{S}_n|,\mathcal{S}_n) = \#\{x : x \in E, \, x \in \mathcal{S}_n\}. \tag{45}$$

Weyl's uniform distribution theorem is extended to the case of a sequence of sets of real numbers in the following way.

Proposition 1: Consider a sequence of the set of real numbers $\{\mathcal{S}_n\}_{n=1}^{\infty}$ such that $|\mathcal{S}_n| < |\mathcal{S}_{n+1}|$ and $|\mathcal{S}_n| \to \infty$, where $|\mathcal{S}_n|$ is the number of elements of $\mathcal{S}_n$. The necessary and sufficient condition that the real numbers $x \in \mathcal{S}_n$ is uniformly distributed asymptotically in the interval $[0,1]$ as $n \to \infty$:

$$\lim_{n \to \infty} \frac{1}{|\mathcal{S}_n|} \sum_{x \in \mathcal{S}_n} \exp[2\pi i m x] = 0, \tag{46}$$

for an arbitrary natural number m.

Proof: The proof is the same line for that of Weyl's uniform distribution theorem.

The condition in Weyl's uniform distribution theorem can be interpreted as

$$\lim_{n \to \infty} \frac{1}{|\mathcal{T}_n|} \sum_{x \in \mathcal{T}_n} \exp[2\pi i m x] = 0,$$

for any natural number m. \tag{47}

Here we defined $\mathcal{T}_n = \cup_{i=1}^{n} \mathcal{S}_i$ and $|\mathcal{T}_n|$ is the number of elements of $\mathcal{T}_n$. The order of the summation over action can be arranged by the symbolic dynamics. For instance, the increasing order of the value of the corresponding digit of given binary sequences is taken. If $|\mathcal{T}_n| > |\mathcal{S}_n|$ and $|\mathcal{S}_n|/|\mathcal{T}_n| \to$ const as $n \to \infty$, we can easily show that Eq. (47) implies

$$\lim_{n \to \infty} \frac{1}{|\mathcal{S}_n|} \sum_{x \in \mathcal{S}_n} \exp[2\pi i m x] = 0,$$

for any natural number m. \tag{48}

Proof: We set $A_n = \Sigma_{x \in \mathcal{T}_n} \exp[2\pi mix]$ and $B_n = \Sigma_{x \in \mathcal{S}_n} \exp[2\pi mix]$. By the triangular inequality, we have

$$\frac{|B_n| - |A_{n-1}|}{|\mathcal{T}_n|} \leq \frac{|A_n|}{|\mathcal{T}_n|}. \tag{49}$$

Thus

$$\frac{|\mathcal{S}_n|}{|\mathcal{T}_n|} \frac{|B_n|}{|\mathcal{S}_n|} \leq \frac{|A_n| + |A_{n-1}|}{|\mathcal{T}_n|} < \frac{|A_n|}{|\mathcal{T}_n|} + \frac{|A_{n-1}|}{|\mathcal{T}_{n-1}|}. \tag{50}$$

The right hand side of Eq. (47) goes to zero. Furthermore,

$|\mathcal{S}_n|/|\mathcal{T}_n|$ tends to a constant value. Therefore, $|B_n|/|\mathcal{S}_n|$ tends to zero.

Let us consider the case of actions of UPOs for the dyadic Baker maps. First, we define $\mathcal{Q}_T \equiv \cup_{i=1}^{T} \mathrm{Fix}(i)$. We identify the set $\mathcal{T}_T$ (or $\mathcal{S}_T$) with $\mathcal{Q}_T$ [or $\mathrm{Fix}(T)$]. We have $|\mathrm{Fix}(T)|/|\mathcal{Q}_T| \to \mathrm{const}$, since the proliferation of periodic orbits is asymptotically determined by the topological entropy. Obviously, $|\mathcal{Q}_n| > |\mathrm{Fix}(n)|$. Therefore, we have the following.

Proposition 2: If the actions of $\cup_{T=1}^{\infty} Fix(T)$ have uniform distribution modulo 1, then actions of $Fix(T)$ has uniform distribution modulo 1 asymptotically.

We have for odd parity,

$$\frac{1}{2|\mathrm{Fix}(T)|} \left| \sum_{S_\nu \in \mathrm{Fix}(T)} \exp[2\pi miS_\nu] + \sum_{S_\nu \in \mathrm{Fix}'(T)} \exp[2\pi miS'_\nu] \right|$$

$$= \frac{1}{2|\mathrm{Fix}(T)|} \left| 2\sinh(\lambda T/2) \frac{1}{2\sinh(\lambda T/2)} \sum_{S_\nu \in \mathrm{Fix}(T)} \exp[2\pi miS_\nu] + 2\cosh(\lambda T/2) \frac{1}{2\cosh(\lambda T/2)} \sum_{S_\nu \in \mathrm{Fix}'(T)} \exp[2\pi miS'_\nu] \right|$$

$$\simeq \frac{1}{2} \frac{1}{2^T} 2\sinh(\lambda T/2) |\mathrm{Tr}(\mathbf{U}^T_{-,m})| = \frac{1}{2} \frac{1}{2^T} 2\sinh(\lambda T/2) \left| \sum_{i=0}^{\infty} \Lambda_i^T(N) \right| \simeq \frac{1}{2} \frac{1}{2^{T/2}} \left| \sum_{i=0}^{\infty} \Lambda_i^T(N) \right| \simeq \frac{1}{2} \left| \exp\left[\left(-\frac{\lambda}{2} + \frac{C}{\sqrt{m}} \right) T \right] \right|$$

$$\to 0 \quad \text{as } T \to \infty, \tag{51}$$

where $\lambda = \ln 2 = 0.693\,14\ldots$ and $C \approx 0.29$. We used the fact that $|\mathrm{Fix}(T)| = 2^T$. By the numerical observation of Ref. 14, this sum converges to 0 as $T \to \infty$. Thus for a dyadic Baker map with symmetry reduction, the actions of the periodic orbits are asymptotically uniform modulo 1 as $T \to \infty$. This fact is consistent with the assumption of Ref. 7. For even parity, we have to change the sign which can be included in the actions S'_ν. After same calculation, we might conclude asymptotically uniformity modulo 1 as $T \to \infty$. However, we think that mathematical rigor is still needed, since the evaluation is crude. To get the uniform distribution modulo 1, the whole of actions should be dense in the unit interval. Now the actions takes rational values. For the dyadic Baker map without symmetry reduction, the behavior of the leading eigenvalues of $\mathbf{U}_N^{(\pm)}$ for even and odd space is important. As mentioned in Ref. 14, the leading eigenvalues of $\mathbf{U}_N^{(\pm)}$ for even and odd space have values of different order. Therefore, we should still carefully discuss about uniform distribution modulo 1 for the case without symmetry reduction.

The extension for a *p*-adic Baker map is done in Appendix C. The actions of UPOs for a *p*-adic Baker map is also rational. If accidental degeneracy often occurs (this probably depends on the value of *p*), by the result of Appendix C, at the present, we cannot say whether the actions of UPOs for the *p*-adic Baker map obey uniform distribution or not, although the numerical observation suggests the uniform distribution modulo 1.

In the next section, we consider the sawtooth map, whose actions can take irrational values for some values of the perturbation parameter *K*.

V. SAWTOOTH MAP

In this section, we consider the sawtooth map. First, we quickly review the classical dynamics of the sawtooth map and show that the expression of the action for periodic orbits has a similar form to that for the Baker maps, namely the one-dimensional Potts spin systems.

Let us start considering the classical dynamics of the sawtooth maps.[27–29] The sawtooth map is defined on a 2-torus. The Hamiltonian is given by

$$H = \frac{y^2}{2} - K\frac{x^2}{2} \sum_{n=-\infty}^{\infty} \delta(t-n), \tag{52}$$

where $\mathcal{D} = [-\frac{1}{2}, \frac{1}{2})$ and $x, y \in \mathcal{D}$. The dynamics is described by the following equation of motion:

$$x_{n+1} = x_n + y_{n+1}, \quad \mathrm{mod}\ 1\ \mathrm{in}\ \mathcal{D},$$
$$y_{n+1} = y_n + Kx_n, \quad \mathrm{mod}\ 1\ \mathrm{in}\ \mathcal{D}. \tag{53}$$

Without modulo operation, we have to introduce the winding number w_x (or w_y) $\in \mathbf{Z}$ along the *x*- (or *y*-) direction, respectively. The mapping now becomes

$$x_{n+1} = x_n + y_{n+1} - w_x^{(n)},$$
$$y_{n+1} = y_n + Kx_n - w_y^{(n)}. \tag{54}$$

Due to the linearity of the sawtooth map, the tangent map for one-step is simply given as

$$M = \begin{bmatrix} K+1 & 1 \\ K & 1 \end{bmatrix}. \tag{55}$$

We define the following quantities for later use:

$$D = K(K+4), \quad \gamma = \frac{K+2+\sqrt{D}}{2},$$ (56)

where γ is the largest eigenvalue of M. The dynamics of the sawtooth map is characterized by the following way: (1) $-4 < K < 0$: The mapping is elliptic. (2) $K < -4$, $0 < K$: The mapping is hyperbolic. The dynamics is totally chaotic. (2-a) K: *Integer* ($K < -4, K > 0$); the sawtooth map becomes Arnold's cat map (Anosov diffeomorphism). It is ergodic. (2-b) K: *Noninteger;* the mapping is discontinuous. This breaks some nice properties which are observed in Arnold's cat maps. However, the system is still ergodic. Even the decay of correlation is exponential. By periodicity, x_n and y_n should be confined in the interval $[-\frac{1}{2}, \frac{1}{2}]$. This enforces the winding number to be bounded by K [see Eq. (54)]. The winding number gives us a natural symbolic description of the trajectory.[27] We define the symbol set $\mathbf{A}$ as $\mathbf{A} = \{-a_{max}(K), -a_{max}(K)+1, ..., -1, 0, 1, ..., a_{max}(K)\}$, where

$$a_{max}(K) = \left[2 + \frac{K}{2}\right],$$ (57)

and $[\cdots]$ represents the integer part of the argument. For the periodic symbolic sequence $\mathbf{s} = s_1 s_2 \cdots s_{T-1} s_T$, the location of periodic points is given by

$$x_n = \frac{\gamma}{(\gamma^2 - 1)(\gamma^T - 1)} \sum_{r=1}^{T} \gamma^{T-r}(\gamma s_{n+r-1} + s_{n-r}),$$ (58)

where $s_i \in \mathbf{A}$. Here we note that in this symbolic description, the mapping from the symbolic sequence $\{s_n\}$ to the position $\{x_n\}$ is one to, at most, one. This property affects the analysis of the quantized maps. The winding numbers of a given periodic orbit along both x- and y-directions can be represented as the sum of the values of positions for the conjugate coordinate, namely

$$w_x = \sum_{n=0}^{T-1} w_x^{(n)} = \sum_{n=0}^{T-1} y_n,$$ (59)

$$w_y = \sum_{n=0}^{T-1} w_y^{(n)} = K \sum_{n=0}^{T-1} x_n.$$ (60)

The action for the periodic orbit with period T is given as[30]

$$S = \sum_{i=0}^{T-1} \left\{ -\left(\frac{y_i^2}{2} - \frac{Kx_i^2}{2}\right) + y_{i+1}(x_{i+1} - x_i) \right.$$

$$\left. - w_y^{(i)} x_i + w_x^{(i-1)} y_i \right\}.$$ (61)

Using Eq. (54) and considering the periodicity carefully, we can show

$$S = \frac{1}{2} \sum_{i=0}^{T-1} (w_x^{(i-1)} y_i - w_y^{(i)} x_i) = \frac{1}{2} \sum_{i=0}^{T-1} \mathbf{x}_i \times \mathbf{w}_i,$$ (62)

where the symbol $\times$ is the exterior product and we define the vectors

$$\mathbf{x}_i \equiv \begin{pmatrix} x_i \\ y_i \end{pmatrix} \quad \text{and} \quad \mathbf{w}_i \equiv \begin{pmatrix} w_x^{(i-1)} \\ w_y^{(i)} \end{pmatrix}.$$ (63)

So the action is the sum of area of triangle with sign. The expression of periodic points can be rewritten into a different form. Here we set $\alpha = \ln \gamma$. Then the periodic point x_n is given by

$$x_n = J(\alpha, T) \sum_{r=0}^{T-1} \cosh\left(\alpha\left(\frac{T}{2} - r\right)\right) s_{n+r},$$ (64)

where

$$J(\alpha, T) = \frac{1}{2 \sinh(\alpha) \sinh(\alpha T/2)}.$$ (65)

The conjugate coordinate for the periodic point becomes

$$y_n = J(\alpha, T) \sum_{r=0}^{T-1} \cosh\left(\alpha\left(\frac{T}{2} - r\right)\right)(s_{n+r} - s_{n+r-1}) + w_x^{(n-1)}.$$ (66)

s_n is expressed in terms of $w_x^{(n)}$ and $w_y^{(n)}$,

$$s_n = w_y^{(n)} + (w_x^{(n)} - w_x^{(n-1)}).$$ (67)

We have an obvious relation,

$$\sum_{i=0}^{T-1} s_i = \sum_{i}^{T-1} w_y^{(i)}.$$ (68)

Inserting Eq. (64) and Eq. (66) into Eq. (62) and using Eq. (68), we finally obtain

$$S = \frac{1}{2} J(\alpha, T) T \sum_{i=0}^{T-1} (w_x^{(i)})^2$$

$$- \frac{1}{2} J(\alpha, T) \sum_{i=0}^{T-1} \sum_{j=0}^{T-1} s_i s_j \cosh\left(\alpha\left(\frac{T}{2} - |i-j|\right)\right).$$ (69)

Equations (62) and (69) are the main result of this section. Compared with the expression, Eq. (12), of the action for the Baker maps, Eq. (69) of the sawtooth maps is the one-dimensional multi-state spin model. Equation (62) expresses the sum of the area of triangles determined by the vectors $\mathbf{x}_i$'s and $\mathbf{w}_i$'s. We also note that the symbolic dynamics for the sawtooth map is not complete, namely there is pruning. These are main differences between the Baker and sawtooth maps. Severe pruning prevents us from carrying out the same procedure of the WPF or Appendix B, since the construction of the integral kernel is impossible. Therefore, we only numerically check the distribution of actions of UPOs.

Action Distribution for Sawtooth Map: We show the results of the numerical studies on action distribution for the sawtooth maps. In order to avoid the number theoretical anomaly, we set the parameter K to be a noninteger. We have done the numerical check of the action distribution for several values. Although we did not find the number theoretical peculiarity for the case that K is a rational value, here we comment that the corresponding quantized map has some anomalous behavior for some rational values of K, such as accidental degeneracy.
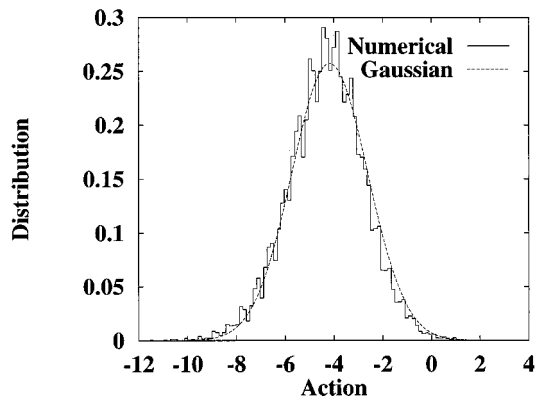
FIG. 9. Action distribution for the sawtooth map with period 9 (K = 3.385756): For higher periods, we can clearly see a periodic oscillation on Gaussian distribution.
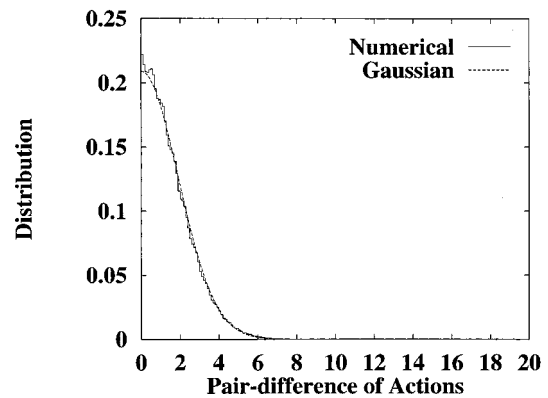

FIG. 11. Distribution of $S_p - S_{p'}$ ($p \neq p'$) for prime periodic orbits (sawtooth map): We only plot the pairs of prime UPOs with period 8 (K = 3.385756). The approximate distribution is Gaussian.

First, we examine the bare action distribution. In Fig. 9, the bare action distribution is depicted for $K = 3.385\,756$ with period from 4 to 9. A remarkable feature is that the distribution is approximately Gaussian with periodic oscillation similar to that as observed for the dyadic (p-adic) Baker maps. We also numerically check the action distribution in modulo 1. It is shown in Fig. 10 and suggests that the fractional parts of the action are uniformly distributed in the unit interval. We also depicted the distribution of the pair-difference of actions. First, we show the bare distribution of the pair-difference of actions in Fig. 11 for the case of period 8. We only show the positive part of the whole distribution. Its distribution is approximated by the Gaussian distribution very well. Second, we show the distribution of the pair-difference of actions in Fig. 12. It suggests that the distribution tends to the uniform distribution.

VI. CONCLUSIONS

We have investigated the statistics of actions of periodic orbits for the (p-adic) Baker map and the sawtooth map. We summarize the results below.

Dyadic Baker map: First, the expression of the action of the Baker map is the Hamiltonian of a one-dimensional lattice gas system. This is very similar to the case of the aniso-

tropic Kepler problem.[17] Reducing geometrical symmetry, we numerically showed that the actions modulo 1 are distributed asymptotically uniformly in the unit interval. Furthermore, replacing the semiclassical trace by some quasiclassical operator introduced by Ref. 15 with a mathematical tool, we showed that the actions modulo 1 are asymptotically uniformly distributed in the unit interval as $T \to \infty$. Therefore, the assumption in Ref. 7 is valid for the dyadic Baker map. However, mathematical rigor is not complete. Actions take rational values. We do not know whether the set of actions is dense in the unit interval or not which is the need for uniform distribution. Therefore, we worry about a possibility of anomaly, like the spectral form factor for the case $N = 2^L$.

Sawtooth map: Similarly, we have shown that the action of periodic orbits for sawtooth maps has the form of the Hamiltonian of a one-dimensional Potts spin model with exponentially decreasing pair-interaction. Unfortunately, the resummation method used for a dyadic Baker map cannot be applied to the sawtooth map, because of severe pruning. Therefore, we only checked the distribution of actions by numerical calculation. We did not show for the case that K is an integer value. For this case, the action systematically degenerates.[31,32] From the numerical observation, in the case
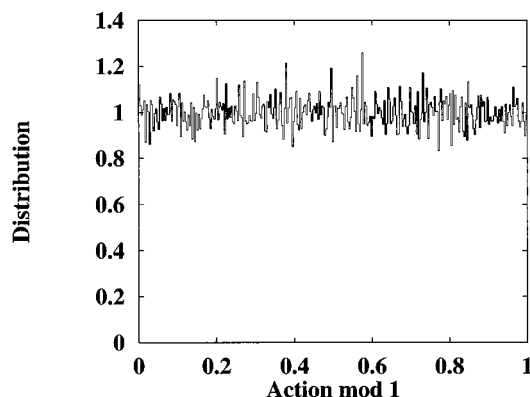

FIG. 10. Action distribution modulo 1 for the sawtooth map with period 9 (K = 3.385756): Approximately, the actions in mod 1 are uniformly distributed in the unit interval.
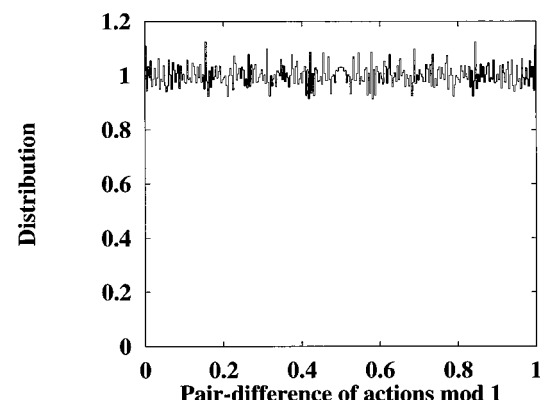

FIG. 12. Distribution of $S_p - S_{p'}$ mod 1 ($p \neq p'$) for prime periodic orbits (sawtooth map): We only plot the pairs of prime UPOs with period 8 (K = 3.385756). The approximate distribution is uniform distribution. But we can clearly see the structure of the fluctuation on the uniform distribution.

that K is not integer, the distribution of actions seems to obey the uniform distribution modulo 1. But the rigorous discussion is still unknown.

Concerning the Riemann zeta function case, the violation of uniform distribution of actions may be a not so surprising fact. The corresponding period now has the form of $\ln p$, where p is prime. The question here is whether the periods satisfy the uniform distribution modulo 1. The interesting result was already obtained:[33] The sequence of $\{\ln p_i\}_{i=1}^{\infty}$ where p_i is the i-th prime, does not satisfy the uniform distribution modulo 1. If we change the order of the summation of $\ln p_i$, we do not know a possibility that a given sequence satisfies the uniform distribution modulo 1. [It is known that if a given sequence $\{a_i\}_{i=0}^{\infty}$ is dense in the unit interval, one can obtain a sequence which satisfies the uniform distribution modulo 1 by changing the order of the summation (Ref. 34).] Irrationality of the actions will be important for the uniform distribution modulo 1. The difference of the statistics of actions between our model considered here and other models such as dispersing billiards or constant negative curvature space, should be investigated.

The expression of actions of the UPOs for a (p-adic) Baker map and sawtooth map has a similar form of one-dimensional spin systems. Also the anisotropic Kepler problem (AKP) which was investigated by Gutzwiller[17] has an approximate expression of actions in terms of the symbolic dynamics derived from a certain hypothesis on symmetry and numerical observation. His hypothetical requirement to the expression of actions is that the action is invariant under the shift and the time-reversal operation. The expression of action of the UPOs for the AKP is very similar to the case of the dyadic Baker map. Here, we speculate that the expression of actions of the UPOs of a given hyperbolic system, which has a well-defined symbolic dynamics, has the form of the Hamiltonian of the one-dimensional spin system. Since the Baker map and sawtooth map are linear, therefore, the expression of actions is just quadratic in symbols. We expect that in general, for nonuniformly hyperbolic systems, the expression of actions has higher-order terms wrt symbols.

ACKNOWLEDGMENTS

APPENDIX A: SEMICLASSICAL EXPRESSION OF $R_2(S)$ (Refs. 6 and 7)

MIT group[6] derived the semiclassical expression of the two-point level correlation function $R_2(s)$. Later Bogomolny and Keating[7] refined the result of Ref. 6 and derived the off-diagonal part by using the bootstrap density of states. The result of Ref. 7 includes the contribution from the repetition of periodic orbits. Here we show that their result for time-broken symmetry classes satisfies the semiclassical sum rule. First, we introduce the result of,[7]

$$R_2(x) = R_2^{(\mathrm{diag})}(x) + R_2^{(\mathrm{off})}(x), \tag{A1}$$

$$R_2^{(\mathrm{diag})}(x) = -\frac{g}{4\pi^2}\frac{\partial^2}{\partial x^2}\ln \mathcal{D}(x), \tag{A2}$$

$$R_2^{(\mathrm{off})}(x) = \frac{\cos(2\pi x)}{2\pi^{2g}}\mathcal{D}^g(x), \tag{A3}$$

where $\hbar = 1$, $\bar{d} = 1$. $g = 1$ and 2 correspond to time-broken symmetry and the time-reversal symmetry classes, respectively. $\mathcal{D}(x)$ is defined by the Perron–Frobenius operator $\mathcal{L}$ for the corresponding classical dynamics. The time-evolution of the density in phase space is determined by

$$(\mathcal{L}^t \rho)(\mathbf{r}) = \int \delta(\mathbf{r} - \Phi^t(\mathbf{r}'))\rho(\mathbf{r}')d\mathbf{r}', \tag{A4}$$

where $\mathbf{r} = (\mathbf{x}, \mathbf{p})$ and Φ is the flow of the classical dynamics. Its Fredholm determinant $Z(z) \equiv \det(1 - e^z \mathcal{L})$ has the zeros as eigenvalues of $\mathcal{L}$. For two-dimensional systems, $Z(z)$ becomes

$$Z(z) = \frac{1}{\zeta(z)} = \prod_p \prod_{k=0}^{\infty}\left(1 - \frac{e^{zT_p}}{|\Lambda_p|\Lambda_p^k}\right)^{k+1} = \prod_{\mu} C_{\mu}(z - \gamma_{\mu}), \tag{A5}$$

where Λ_p is the maximum eigenvalue of the monodromy matrix M_p and $\{\gamma_{\mu}\}$ is the Pollicott–Ruelle resonances ($\{e^{-\gamma_{\mu}}\}$ is the eigenvalues of $\mathcal{L}$) and $\gamma_0 = 0$ is the equilibrium state. Remark that for mixing systems, for $\mu \neq 0$, $\Re\gamma_{\mu} > 0$. $\mathcal{D}(x)$ is given by

$$\mathcal{D}(x) = |\mathcal{N}\zeta(ix)|^2 = \prod_{\mu}\frac{A_{\mu}^2}{x^2 + \gamma_{\mu}^2}, \tag{A6}$$

where $\mathcal{N}$ is the normalization factor and A_{μ} is the regularization factor,

$$A_{\mu} = \begin{cases} 1, & \mu = 0, \\ \gamma_{\mu}, & \mu \neq 0. \end{cases} \tag{A7}$$

In Ref. 7, they derived the correction from the repetition of periodic orbits for the above MIT result.

Next we check the validity of the semiclassical sum rule for the above semiclassical expression of $R_2(s)$. For time-broken symmetry classes, we have

$$\lim_{\epsilon \to 0} 2\pi\epsilon\langle(d_{\epsilon}(E))^2\rangle$$

$$= \lim_{\epsilon \to 0} 2\pi\epsilon R_2^{\epsilon}(x = 0)$$

$$= \lim_{\epsilon \to 0} 2\pi\epsilon\frac{1}{2\pi^2}\left\{\frac{1}{4\epsilon^2} + \sum_{\mu \neq 0}\frac{\gamma_{\mu}^2 + 4\epsilon^2}{(\gamma_{\mu}^2 - 4\epsilon^2)^2}\right.$$

$$\left. - \frac{1}{4\epsilon^2}(1 - 4\pi d_0\epsilon + \cdots)\prod_{\mu \neq 0}\frac{1}{1 - 4\epsilon^2/\gamma_{\mu}^2}\right\}$$

$$= \lim_{\epsilon \to 0}\frac{\epsilon}{\pi}\left\{\frac{\pi d_0}{\epsilon} + \mathcal{O}(\epsilon^0)\right\} = d_0 = \langle d(E)\rangle. \tag{A8}$$

Therefore, the semiclassical sum rule is satisfied. This is rather astonishing result, since it is believed that the semiclassical theory does not explain the limit of $t \to \infty$ ($s \to 0$). (Remark that there is no need for the contribution from the repetition of periodic orbits.) For time-reversal symmetry classes, we get

$$\lim_{\epsilon \to 0} 2 \pi \epsilon \langle (d_\epsilon(E))^2 \rangle$$

$$= \lim_{\epsilon \to 0} 2 \pi \epsilon R_2^\epsilon(x=0)$$

$$= \lim_{\epsilon \to 0} 2 \pi \epsilon \left[-\frac{1}{\pi^2} \left(\frac{1}{(2 i \epsilon)^2} + \sum_{\mu \neq 0} \frac{\gamma_\mu^2 - (2 i \epsilon)^2}{((2 i \epsilon)^2 + \gamma_\mu^2)^2} \right) \right.$$

$$\left. + \frac{\cosh(4 \pi \epsilon)}{2 \pi^4} \frac{1}{(2 i \epsilon)^4} \prod_{\mu \neq 0} \left(\frac{1}{1 + (2 i \epsilon)^2 / \gamma_\mu^2} \right)^2 \right] = \infty. \quad (A9)$$

It fails the semiclassical sum rule. In Ref. 13, the time-reversal symmetry breaking of $R_2(s)$ was considered. But in no AB-flux limit (time-reversal limit), it still has a problem.

APPENDIX B: GUTZWILLER'S RESUMMATION METHOD

In order to evaluate the semiclassical trace $\mathrm{Tr}^{(\mathrm{sc})}(B^T)$, we employ the Gutzwiller's resummation method[17] to quantized dyadic Baker's maps, which was used for the AKP. His method is essentially the use of Kac's method[35,36] to the one-dimensional Ising spin problem with the interaction of exponentially decreasing function. The action for the dyadic Baker's map has been already given in Eq. (17). We rewrite this into the following form:

$$\bar{S}_\nu = \frac{1}{4} M_\nu + \frac{1}{4 \sinh(\lambda T/2)} \sum_{i,j} a_i a_j \cosh \left(\lambda \left(\frac{T}{2} - |i-j| \right) \right). \quad (B1)$$

Since the phase factors in the trace appear as $\exp(2 \pi N S_\nu i)$, we can drop $\frac{1}{4} M_\nu$ for sufficiently large N with $N = 2^L$. Then we have

$$\bar{S}_\nu = \frac{1}{2} \mathbf{x}_\nu^\mathsf{T} \cdot \mathbf{A} \cdot \mathbf{x}_\nu, \quad (B2)$$

where

$$\mathbf{x}_\nu = (a_0, a_1, \ldots, a_{T-1})^\mathsf{T}, \quad (B3)$$

and the matrix elements $\mathbf{A}_{ij}$ is given as

$$\mathbf{A}_{ij} = \frac{1}{2 \sinh(\lambda T/2)} \cosh \left(\lambda \left(\frac{T}{2} - |i-j| \right) \right). \quad (B4)$$

Here we denote $\mathbf{B} = \mathbf{A}^{-1}$ the inverse of $\mathbf{A}$. One can show that

$$\mathbf{B} = \begin{vmatrix} \alpha & \beta & 0 & \cdots & 0 & \beta \\ \beta & \alpha & \beta & & & 0 \\ 0 & \beta & \alpha & \ddots & & \vdots \\ \vdots & & \ddots & \ddots & \ddots & 0 \\ 0 & & & \ddots & \alpha & \beta \\ \beta & 0 & \cdots & 0 & \beta & \alpha \end{vmatrix}, \quad (B5)$$

where

$$\alpha = 2 \coth(\lambda) \quad \text{and} \quad \beta = -\frac{1}{\sinh(\lambda)}. \quad (B6)$$

The determinants $\det(\mathbf{A})$ and $\det(\mathbf{B})$ are given as

$$\det(\mathbf{A}) = \frac{e^{-\lambda T}}{2} \frac{\sinh(\lambda T)}{[\sinh(\lambda T/2)]^2} \quad \text{and} \quad \det(\mathbf{B}) = \det(\mathbf{A})^{-1}. \quad (B7)$$

Here we rewrite the action $\bar{S}_\nu$ in terms of the variables $\sigma_i \in \{-1, 1\}$, instead of the variables a_i,

$$\mathbf{x}_\nu = \frac{1}{2}(\mathbf{1} + \boldsymbol{\sigma}) \quad \text{and} \quad \boldsymbol{\sigma} = (\sigma_0, \ldots, \sigma_{T-1})^\mathsf{T} \quad \text{and} \quad \mathbf{1} = (1, \ldots, 1)^\mathsf{T}. \quad (B8)$$

Then we have

$$\bar{S}_\nu = \frac{1}{8} \mathbf{1}^\mathsf{T} \cdot \mathbf{A} \cdot \mathbf{1} + \frac{1}{4} \boldsymbol{\sigma}^\mathsf{T} \cdot \mathbf{A} \cdot \mathbf{1} + \frac{1}{8} \boldsymbol{\sigma}^\mathsf{T} \cdot \mathbf{A} \cdot \boldsymbol{\sigma}. \quad (B9)$$

We can easily check that

$$\sum_{j=1}^T A_{ij} = \frac{3}{2} \quad \text{and} \quad \sum_{j=1}^T A_{ij} = \sum_{j=1}^T A_{i'j} \quad \text{for} \quad i \neq i'. \quad (B10)$$

Thus we can omit the first two terms in Eq. (B9) for sufficiently large $N = 2^L$. After all, we arrive at

$$\frac{i}{\hbar} \bar{S}_\nu = \frac{1}{2} \boldsymbol{\sigma}^\mathsf{T} \cdot \mathcal{A} \cdot \boldsymbol{\sigma}, \quad (B11)$$

where $\mathcal{A} = (s/4) \mathbf{A}$ and $s = i/\hbar$. Therefore, for $N = 2^L$ (L; sufficiently large), we have

$$\mathrm{Tr}^{(\mathrm{sc})}(B^T) = \frac{1}{2 \sinh(\lambda T/2)} \sum_\nu \exp \left[\frac{1}{2} \boldsymbol{\sigma}^\mathsf{T} \cdot \mathcal{A} \cdot \boldsymbol{\sigma} \right]. \quad (B12)$$

Now we apply the following Hubbard–Stratonovich transform to Eq. (B12),

$$\exp \left[\frac{1}{2} \boldsymbol{\sigma}^\mathsf{T} \cdot \mathcal{A} \cdot \boldsymbol{\sigma} \right]$$

$$= (2 \pi)^{-T/2} (\det(\mathcal{C}))^{1/2} \int_{-\infty}^{\infty} dz_1 \cdots \int_{-\infty}^{\infty} dz_T$$

$$\times \exp \left[-\frac{1}{2} \mathbf{z}^\mathsf{T} \cdot \mathcal{C} \cdot \mathbf{z} \right] \exp[\boldsymbol{\sigma}^\mathsf{T} \cdot \mathbf{z}], \quad (B13)$$

where $\mathcal{A}$ and $\mathcal{C}$ are real positive definite symmetric $T \times T$ matrices and $\mathcal{A}^{-1} = \mathcal{C}$. Here we suppose that s is a real positive number. After the transformation, we analytically continue the result in the complex domain as done in Ref. 17. Employing the Hubbard–Stratonovich transform, we have

$$\mathrm{Tr}^{(sc)}(B^T) = \mathcal{F}(T,N) \int_{-\infty}^{\infty} dz_1 \cdots \int_{-\infty}^{\infty} dz_T$$

$$\times \exp\left[-\frac{1}{2} \mathbf{z}^T \cdot \mathcal{C} \cdot \mathbf{z} + \sum_{i=1}^{T} \ln(\cosh(z_i)) \right],$$

(B14)

where

$$\mathcal{F}(T,N) = \frac{2^T}{2 \sinh(\lambda T/2)} (2\pi)^{-T/2} (\det(\mathcal{C}))^{1/2}. \qquad (B15)$$

The argument of the exponential function in the integrand of Eq. (B14) is rewritten as

$$\sum_{i=1}^{T} \left\{ -\frac{2}{s} \left[\tanh\left(\frac{\lambda}{2}\right)(z_i^2 + z_{i+1}^2) + \mathrm{cosech}(\lambda)(z_i - z_{i+1})^2 \right] \right.$$

$$\left. + \ln \cosh(z_i) \right\}. \qquad (B16)$$

We scale $z_i = R\xi_i$, where $R = \sqrt{s/8}$. Then we have

$$\mathrm{Tr}^{(sc)}(B^T) = \mathcal{G}(T) \mathrm{Tr}(\mathcal{K}^T), \qquad (B17)$$

where

$$\mathcal{G}(T) = \left[\frac{(2 \sinh(\lambda))^T}{2 \sinh(\lambda T)} \right]^{1/2} e^{\lambda T} \qquad (B18)$$

and

$$\mathcal{K}(\xi, \eta) = \sqrt{\cosh(R\xi)} \, \frac{\exp[-(1/4)\{\tanh(\lambda/2)(\xi^2 + \eta^2) + \mathrm{cosech}(\lambda)(\xi - \eta)^2\}]}{\sqrt{2\pi 2 \sinh(\lambda)}} \sqrt{\cosh(R\eta)}, \qquad (B19)$$

and

$$\mathrm{Tr}(\mathcal{K}^T) = \int_{-\infty}^{\infty} d\xi_1 \cdots \int_{-\infty}^{\infty} d\xi_T \prod_{i=1}^{T} \mathcal{K}(\xi_i, \xi_{i+1}). \qquad (B20)$$

Here we impose the periodic boundary condition $\xi_{T+1} = \xi_1$. The expression obtained has the same form as that for the anisotropic Kepler problem except some coefficients. Remark that the factor $\mathcal{G}(T)$ asymptotically behaves as

$$\mathcal{G}(T) \sim e^{\lambda T}, \quad \text{as} \quad T \to \infty. \qquad (B21)$$

The eigenvalue problem of the kernel $\mathcal{K}(\xi, \eta)$ is

$$\int_{-\infty}^{\infty} \mathcal{K}(x,y) \psi(y) \, dy = \mu \psi(x). \qquad (B22)$$

We denote $\{\mu_i\}_{i=1}^{\infty}$ the set of eigenvalues of the kernel $\mathcal{K}(\xi, \eta)$ and assume that $\{\mu_i\}_{i=0}^{\infty}$ are ordered as

$$|\mu_0| > |\mu_1| \geqslant |\mu_2| \geqslant \cdots > 0. \qquad (B23)$$

Then we have

$$\mathrm{Tr}^{(sc)}(B^T) = \mathcal{G}(T) \sum_{i=0}^{\infty} \mu_i^T. \qquad (B24)$$

Therefore, our next task is to evaluate the leading eigenvalue μ_0 of the kernel $\mathcal{K}(\xi, \eta)$. However, unfortunately, the obtained kernel diverges in the semiclassical limit $\hbar \to 0$. See Eq. (B19). Thus, we cannot use for the analysis unlike the quasiclassical operator $\mathbf{U}_N$.[15,14]

APPENDIX C: EXTENSION TO *p*-ADIC BAKER MAP

In this section, we consider the case of *p*-adic Baker maps and examine the behavior of the action distribution compared with the case of dyadic Baker maps. The extension to the *p*-adic Baker map is straightforward. The mapping is now given as

$$x' = px - [px], \quad y' = \frac{y + [px]}{p}, \qquad (C1)$$

where $p \geqslant 2 \in \mathbf{N}$. In a similar way to the dyadic Baker map, we have the action for the periodic orbit with period T,

$$S_\nu^{(p)} = \frac{\nu \bar{\nu}}{p^T - 1}, \qquad (C2)$$

where

$$\nu = \sum_{i=0}^{T-1} a_i p^{T-i-1}, \quad \bar{\nu} = \sum_{i=0}^{T-1} a_i p^i, \qquad (C3)$$

and $a_i, b_i \in \{0,1,\ldots,p-1\}$. Since we take the modulo operation, for simplicity, we can remove some integer from $S_\nu^{(p)}$, and thus define
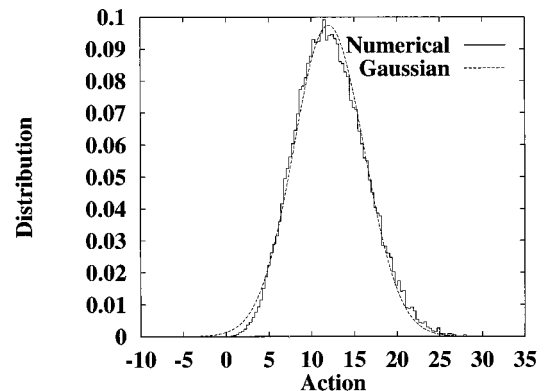

FIG. 13. Action distribution of the expression $S_\nu = \Sigma x_i a_i$ for the *p*-adic Baker map ($p=5$): for the prime periodic orbits with period 9. Clearly, the approximate distribution is Gaussian. The distribution has a periodic oscillation.
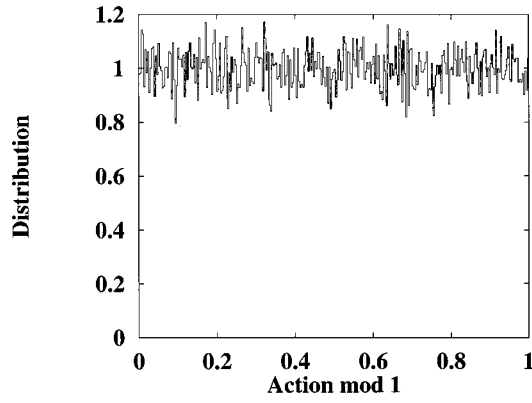
FIG. 14. Action distribution in modulo 1 for the p-adic Baker map ($p=5$): for the prime periodic orbits with period 9. Clearly, the limiting distribution is uniform distribution.

$$\overline{S_\nu^{(p)}} = \sum_{i=0}^{T-1} x_i a_i$$

$$= \frac{e^{\lambda_p[(T/2)-1]}}{2\sinh(\lambda_p T/2)} \left\{ \sum_{i=0}^{T-1} a_i^2 + e^{-\lambda_p T/2} \sum_{i\neq j} a_i a_j \right.$$

$$\left. \times \cosh\left[\lambda_p\left(\frac{T}{2}-|i-j|\right)\right]\right\}, \qquad (C4)$$

where $\lambda_p = \ln p$. The expression of the action $\overline{S_\nu^{(p)}}$ is now the Hamiltonian of the one-dimensional multi-state lattice gas.

In Fig. 13, the action distribution for the expression, Eq. (C4) is depicted for the case $p=5$ with period from 6 to 9. Compared with the dyadic case, the distribution of the p-adic case with a larger value of $p(p\geqslant 3)$ tends to the Gaussian distribution more smoothly, since the gap between peaks is narrower for large p. Then we speculate that the dyadic case is very anomalous. Remember that the number 2 is a special integer in number theory. We also numerically check the action distribution in modulo 1 for the expression, Eq. (C4) (Fig. 14). It seems that the limiting distribution is the uniform distribution. The pair-difference of the actions is also numerically checked. It seems that the bare distribution of the pair-difference of the actions tends to the Gaussian distribution [Fig. 15(a)] and that in modulo 1 tends to the uniform distribution [Fig. 15(b)]. At present, we do not find number theoretical peculiarities for $p\geqslant 3$.

The quantized p-adic Baker map and its semiclassical analysis are also similarly constructed,

$$B_p = G_N^{-1} \begin{pmatrix} G_{N/p} & 0 & \cdots & \cdots & 0 \\ 0 & G_{N/p} & \ddots & \cdots & 0 \\ \vdots & \ddots & \ddots & \ddots & \vdots \\ 0 & \cdots & \ddots & G_{N/p} & 0 \\ 0 & \cdots & \cdots & 0 & G_{N/p} \end{pmatrix}, \quad (C5)$$
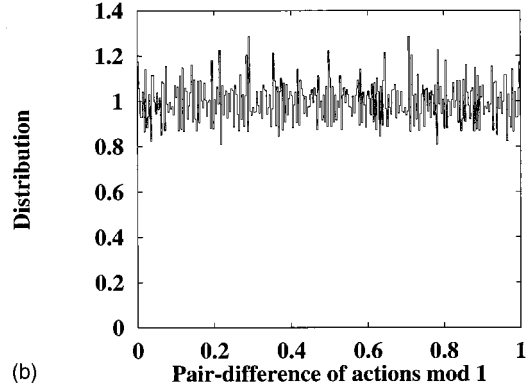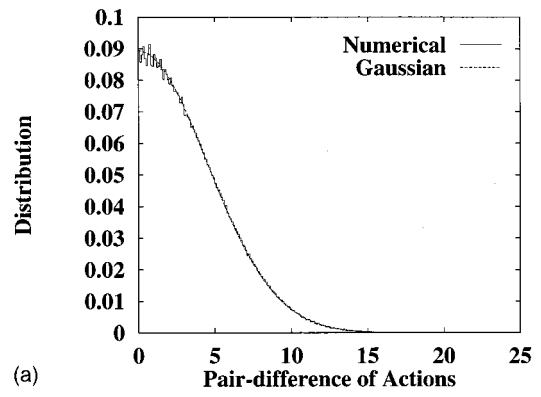

FIG. 15. Distribution of the pair-difference of actions $[S_\nu^{(p)} - S_{\nu'}^{(p)}(\nu \neq \nu')]$ of prime periodic orbits for a p-adic Baker map ($p=5$, period $T=6$): (a) The bare distribution of the pair-difference of actions. We only show the positive part of the whole distribution. The envelope function seems to be the Gaussian distribution. (b) The distribution in modulo 1. The approximate distribution is uniform distribution.

where $N \in p\mathbf{N}$. The semiclassical trace of B_p is given as

$$\mathrm{Tr}^{(\mathrm{sc})}(B_p^T) = \frac{1}{2\sinh(\lambda_p T/2)} \sum_\nu \exp[2\pi N i S_\nu^{(p)}], \qquad (C6)$$

where $\lambda_p = \ln p$. In a similar way to the dyadic Baker map, after a cumbersome calculation due to the Hubbard–Stratonovich transform, we have the semiclassical trace (for $16p|N$),

$$\mathrm{Tr}^{(\mathrm{sc})}(B_p^T) = \mathcal{G}_p(T) \mathrm{Tr}(\mathcal{K}_p^T), \qquad (C7)$$

where

$$\mathcal{G}_p(T) = \left[\frac{(2\sinh(\lambda_p))^T}{2\sinh(\lambda_p T)}\right]^{1/2} e^{\lambda_p T} \qquad (C8)$$

and

$$\mathcal{K}_p(\xi,\eta) = \sqrt{h(R_p\xi;p)} \; \frac{\exp[-(1/4)\{\tanh(\lambda_p/2)(\xi^2+\eta^2)+\operatorname{cosech}(\lambda_p)(\xi-\eta)^2\}]}{\sqrt{2\pi2\sinh(\lambda_p)}} \; \sqrt{h(R_p\eta;p)}, \tag{C9}$$

and

$$h(z;p) = \begin{cases} \displaystyle\sum_{r=0}^{l-1} \cosh\big((2l-2r-1)z\big), & p=2l: \text{even}, \\[2ex] \displaystyle\sum_{r=0}^{l-1} \cosh\big(2(l-r)z\big)+(1/2), & p=2l+1: \text{odd}, \end{cases} \tag{C10}$$

and $R_p=\sqrt{s/8}$. In view of the field theory, the potential which comes from the sum over all spin configurations is not $\ln\cosh(R_p\xi)$. This and the value of λ_p are the main differences between the dyadic Baker map and p-adic Baker map. This kernel $\mathcal{K}_p(\xi,\eta)$ also diverges in the semiclassical limit $\hbar\to0$. Thus, we cannot employ the analysis unlike the case of the quasiclassical operator introduced by Ref. 15.

[1] R. Artuso, E. Aurell, and P. Cvitanović, Nonlinearity **3**, 325 (1990); **3**, 361 (1990).
[2] P. Cvitanović and B. Eckhardt, J. Phys. A **24**, L237 (1991).
[3] W. Parry and M. Pollicott, Ann. Math. **118**, 573 (1983).
[4] T. Harayama and A. Shudo, J. Phys. A **25**, 4595 (1992).
[5] P. Dahlqvist, J. Phys. A **28**, 4733 (1995).
[6] O. Agam, B. Altshuler, and A. V. Andreev, Phys. Rev. Lett. **75**, 4389 (1995).
[7] E. B. Bogomolny and J. P. Keating, Phys. Rev. Lett. **77**, 1472 (1996).
[8] M. V. Berry, Proc. R. Soc. London, Ser. A **400**, 229 (1985).
[9] J. H. Hannay and A. M. Ozorio de Almeida, J. Phys. A **17**, 3429 (1984).
[10] N. Argaman, E. Doron, J. Keating, A. Kitaev, M. Sieber, and U. Smilansky, Phys. Rev. Lett. **71**, 4326 (1993).
[11] J. P. Keating, ''The semiclassical sum rule and Riemann's zeta function,'' in *Quantum Chaos,* edited by H. A. Carderia, R. Ramaswamy, M. C. Gutzwiller, and G. Casati (World Scientific, Singapore, 1992), p. 28.
[12] J. P. Keating, ''The Riemann zeta function and quantum chaology,'' in *Quantum Chaos,* edited by G. Casati, I. Guarneri, and U. Smilansky (North-Holland, Amsterdam, 1993), p. 145.
[13] M. M. Sano, J. Phys. Soc. Jpn. **67**, 2678 (1998).
[14] G. Tanner, J. Phys. A **32**, 5071 (1999).
[15] F-M. Dittes, E. Doron, and U. Smilansky, Phys. Rev. E **49**, R963 (1994).
[16] A. M. Ozorio de Almeida and M. Saraceno, Ann. Phys. (New York) **210**, 1 (1991).
[17] M. C. Gutzwiller, Physica D **5**, 183 (1982).
[18] N. L. Balazs and A. Voros, Europhys. Lett. **4**, 1089 (1987); Ann. Phys. (New York) **190**, 1 (1989)
[19] M. Saraceno, Ann. Phys. (New York) **199**, 37 (1990).
[20] E. B. Bogomolny, B. Gerogeot, M.-J. Giannoni, and C. Schmidt, Phys. Rep. **291**, 219 (1997).
[21] M. Saraceno and A. Voros, Physica D **79**, 206 (1994).
[22] A. Lakshminarayan, Ann. Phys. (New York) **239**, 272 (1995).
[23] J. P. Keating, J. Phys. A **27**, 6605 (1994).
[24] First, we tried to estimate the semiclassical trace by the resummation method of Gutzwiller. However, in the semiclassical limit, Gutzwiller's method fails. Then we changed the plan. See Appendix B in details.
[25] A. Shudo and K. Ikeda, Prog. Theor. Phys. Suppl. **116**, 283 (1994).
[26] H. Weyl, Math. Ann. **77**, 313 (1916).
[27] I. Pecival and F. Vivaldi, Physica D **27**, 373 (1987); N. Bird and F. Vivaldi, *ibid.* **30**, 164 (1988).
[28] S. Vaienti, J. Stat. Phys. **67**, 251 (1992).
[29] N. I. Chernov, J. Stat. Phys. **69**, 111 (1992).
[30] M. M. Sano, J. Phys. A **29**, 6087 (1996).
[31] J. H. Hannay and M. V. Berry, Physica D **1**, 267 (1980).
[32] J. P. Keating, Nonlinearity **4**, 277 (1991); **4**, 309 (1991).
[33] A. Wintner, Q. J. Math. **6**, 65 (1935).
[34] L. Kuipers and H. Niederreiter, *Uniform Distribution of Sequences* (Wiley, New York, 1974).
[35] M. Kac, Phys. Fluids **2**, 8 (1959).
[36] M. Kac, in *Statistical Physics: Phase Transitions and Superfluidity*, Brandeis University Summer Institute in Theoretical Physics, 1966 (Gordon and Breach, New York, 1968), Vol. 1, pp. 241–305.
[37] For numerical calculation, REISPACK and GRAPHYS were used. REISPACK and GRAPHYS were written by Dr. S. Adachi.